

# Developing diagnostic tools for low-burnup reactor samples

Patrick Jaffke,<sup>1,\*</sup> Benjamin Byerly,<sup>1,2</sup> Jamie Doyle,<sup>1</sup> Anna Hayes,<sup>1</sup> Gerard Jungman,<sup>1</sup> Steven Myers,<sup>1</sup> Angela Olson,<sup>1</sup> Donivan Porterfield,<sup>1</sup> and Lav Tandon<sup>1</sup>

<sup>1</sup>*Los Alamos National Laboratory, Los Alamos, NM 87545, USA*

<sup>2</sup>*Department of Geology and Geophysics, Louisiana State University, Baton Rouge, LA 70803, USA*

(Dated: September 18, 2018)

We test common fluence diagnostics in the regime of very low burnup natural uranium reactor samples. The fluence diagnostics considered are the uranium isotopes ratios  $^{235}\text{U}/^{238}\text{U}$  and  $^{236}\text{U}/^{235}\text{U}$ , for which we find simple analytic formulas agree well with full reactor simulation predictions. Both ratios agree reasonably well with one another for fluences in the mid  $10^{19} \text{ n/cm}^2$  range. However, below about  $10^{19} \text{ n/cm}^2$  the concentrations of  $^{236}\text{U}$  are found to be sufficiently low that the measured  $^{236}\text{U}/^{235}\text{U}$  ratios become unreliable. We also derive and test diagnostics for determining sample cooling times in situations where very low burnup and very long cooling times render many standard diagnostics, such as the  $^{241}\text{Am}/^{241}\text{Pu}$  ratio, impractical. We find that using several fragment ratios are necessary to detect the presence of systematic errors, such as fractionation.

## I. ISOTOPICS INTRODUCTION

Determining the reactor environment that a particular spent fuel sample experienced is critical information for non-proliferation and reactor verification. In particular, the fluence is often related to the fuel burnup and, hence, the plutonium production and grade [1]. This makes the fluence an important parameter for non-proliferation and arms reduction [2]. The fluence of a sample can be inferred in many ways, but is most commonly derived from isotopic ratios of actinides, such as  $^{235}\text{U}/^{238}\text{U}$  or  $^{236}\text{U}/^{235}\text{U}$  [3, 4] and various plutonium ratios [5]. Additional methods utilize the ratios of activated isotopes in cladding and moderator material, such as the graphite isotope ratio method (GIRM) [6–8], or of ratios of long-lived fragments such as cesium [5, 9, 10], europium [9], or neodymium [5]. The cooling time is often determined with ratios utilizing short-lived actinides, such as  $^{241}\text{Pu}/^{241}\text{Am}$  [11], but can also be inferred by gamma spectroscopy of fragments [12]. The cooling time provides one with an estimate of the sample age, which is also pertinent for forensics and nonproliferation.

One can determine the final activities, abundances, and ratios of nuclides with detailed reactor simulations, provided a burnup history and initial fuel composition. Our goal is to invert this process, where one begins with measured isotopic abundances or ratios and then determines the reactor parameters, such as the fluence and cooling time. We focus on these two parameters as they are derived from so-called linear systems, which have simpler analytical forms, in the low burnup regime. Non-linear systems can be used to infer parameters, such as the flux and shutdown history [13]. In our regime of interest, new cooling time diagnostics are developed and verified alongside the standard fluence diagnostics. Several cooling time diagnostics are utilized to detect the presence of systematic errors. We used low burnup

archived samples, available at Los Alamos National Laboratory, to test these diagnostics. The chemical analyses to determine the abundances of the actinides and fission fragments for our low burnup samples can be found in Ref. [14] and Ref. [15].

This paper is structured as follows. The fluence diagnostics are discussed in Sec. II. Cooling time diagnostics are discussed and derived in Sec. III. The diagnostics are verified with reactor simulations and theoretical errors are generated in Sec. IV. The diagnostics are then applied to low burnup reactor samples to determine their fluence, cooling time, and sensitivity to systematic errors in Sec. V. We conclude in Sec. VI.

## II. FLUENCE DIAGNOSTICS

The fluence diagnostics considered in this work utilize the uranium isotopic ratios:  $^{235}\text{U}/^{238}\text{U}$  and  $^{236}\text{U}/^{235}\text{U}$ . Ratios utilizing moderator materials require a sample removal from the existing reactor, which is often not feasible or impacts future reactor design and safety. In addition, some long-lived fragments, such as  $^{134}\text{Cs}$  or  $^{154}\text{Eu}$ , are produced in extremely low concentrations for low burnup scenarios creating experimental difficulties. Finally,  $^{239}\text{Pu}$  cannot be used, as its accumulation is not precisely linear in fluence in low burnup scenarios, thus displaying a flux dependence. For these reasons, we focus on the uranium ratios above which are trivially related to the fluence via

$$\begin{aligned} \epsilon(\Phi, \epsilon_0) &= \epsilon_0 e^{-\Phi(\sigma_{U235}^T - \sigma_{U238}^T)} \\ \rho(\Phi) &= \left( \frac{\sigma_{U235}^c}{\sigma_{U236}^T - \sigma_{U235}^T} \right) \left( 1 - e^{-\Phi(\sigma_{U236}^T - \sigma_{U235}^T)} \right). \end{aligned} \quad (1)$$

Here,  $\epsilon$  denotes the  $^{235}\text{U}/^{238}\text{U}$  ratio and  $\rho$  the  $^{236}\text{U}/^{235}\text{U}$  ratio. The superscripts on the cross-sections  $\sigma$  are for

\* corresponding author: pjaffke@lanl.gov

capture ( $c$ ) or total ( $T$ ) reactions and  $\Phi$  is the fluence <sup>1</sup>.

We immediately note that  $\epsilon$  depends on the initial ratio  $\epsilon_0$ . This implies that a measurement of  $\Phi$  via the  $^{235}\text{U}/^{238}\text{U}$  ratio is only valid when the initial enrichment is known. In the case of our low burnup samples, all indicated natural uranium (NU) as the initial fuel [14]. On the other hand, the determination of  $\Phi$  from  $\rho$  is insensitive to the initial fuel, but requires a measurement of  $^{236}\text{U}$ , which is produced in very low quantities when the burnup is low. A final note is that a measurement of  $\Phi$  using Eq. 1 will be most sensitive to the thermal fluence, as these cross-sections dominate (specifically  $^{235}\text{U}$  thermal fission).

Inverting Eq. 1 produces the fluence diagnostics we will apply to the low burnup samples

$$\Phi = \frac{\ln(\epsilon_0/\epsilon)}{\sigma_{U235}^T - \sigma_{U238}^T}$$

$$\Phi = \frac{1}{\sigma_{U235}^T - \sigma_{U236}^T} \ln \left( \frac{\sigma_{U235}^c - \rho(\sigma_{U236}^T - \sigma_{U235}^T)}{\sigma_{U235}^c} \right). \quad (2)$$

Measurement of the values of  $\epsilon$  or  $\rho$  are typically accomplished by chemical separation [16–18], followed by gamma spectroscopy [5], thermal ionization mass spectrometry (TIMS) [14], or inductively coupled plasma mass spectrometry (ICP-MS) [3, 4]. Specifically, the measurement of  $^{236}\text{U}$  is made difficult as isobaric interferences arise when small quantities of  $^{236}\text{U}$  exist amidst large  $^{235}\text{U}$  and  $^{238}\text{U}$  quantities. Additionally, the  $\alpha$ -decay peak of  $^{235}\text{U}$  can interfere in a  $^{236}\text{U}/^{238}\text{U}$  measurement done via  $\alpha$ -spectrometry [19, 20].

### III. COOLING TIME DIAGNOSTICS

Cooling time diagnostics must be selected specifically for the context of low burnup samples. For example, the  $^{241}\text{Pu}/^{241}\text{Am}$  ratio cannot be used as neither  $^{241}\text{Pu}$  nor  $^{241}\text{Am}$  are produced in appreciable amounts at low burnups. Similar issues preclude the use of other unstable actinides from NU fuel or  $^{134}\text{Cs}$  and  $^{154}\text{Eu}$ , both of which are non-linear nuclides [21] that rely on neutron capture as their primary production channel. This indicates that common cooling time diagnostics that utilize same-species ratios to avoid fractionation [22], such as the  $^{134}\text{Cs}/^{137}\text{Cs}$  ratio [23], are invalid. In addition, the special case of extremely long cooling times <sup>2</sup> ( $\sim 20$  yr) invalidate the use of some major decay heat tags, such as  $^{106}\text{Ru}$  and  $^{144}\text{Ce}$  [24]. Thus, the cooling time diagnostic requires nuclides that are appreciably produced in

low burnup scenarios, have long half-lives, and are easy to chemically separate and analyze. These requirements naturally lead one to the so-called ‘linear’ fission fragments, described by:

1. The linear fragment  $N_L$  has a halflife such that its decay constant  $\lambda_L$  satisfies  $\lambda_L T_{\text{irr}} \ll 1$ .
2. The fission product cumulative yields for  $N_L$  are large.
3. The beta-parents of  $N_L$  have halflives such that they are in equilibrium during  $T_{\text{irr}}$ .

These fragments are dubbed ‘linear’ as their production is linear in the fluence  $\Phi = \phi T_{\text{irr}}$ . The first criteria ensures that the fragment is long-lived relative to the irradiation period of the reactor. The second criteria demands that the fragment is appreciably produced in fission. The third criteria allows one to derive a simple analytical expression for  $N_L$ , independent of its  $\beta$ -parents. For our low burnup purposes,  $^{85}\text{Kr}$ ,  $^{125}\text{Sb}$ ,  $^{137}\text{Cs}$ , and  $^{155}\text{Eu}$  are linear fragments. Next, we proceed to derive the simple expressions for these and verify that they satisfy the criteria above with detailed reactor simulations.

All nuclides in a reactor environment are governed by depletion equations, which form the basis for constructing an interaction matrix between the various nuclides. This is the structure utilized by many reactor simulation codes [25, 26], which often solve these massive ( $\sim 2000$  species) systems as an eigenvalue problem [27]. In our case, we can utilize linear fragments to construct a simple isolated system, which resembles a Bateman equation [28],

$$\frac{dN_L}{dt} = -\tilde{\lambda}_L N_L + \vec{Z}_L \cdot \vec{\mathcal{F}}. \quad (3)$$

The positive (negative) terms denote production (depletion) channels and we use an effective decay constant  $\tilde{\lambda} = \lambda + \phi \sigma^T$ . We note that the full depletion equation, which resembles Eq. 1 of Ref. [29], reduces to Eq. 3 after applying  $\lambda_i \gg b_{j,i} \lambda_j$  (criteria 3), noting that  $\sigma_{j,i} \phi \ll b_{j,i} \lambda_j$  is satisfied for most fragments <sup>3</sup>, and adding an explicit fission term. Thus, Eq. 3 states that a linear fragment  $N_L$  is produced in fission with a fission rate vector  $\vec{\mathcal{F}}$  and a cumulative yield  $\vec{Z}_L$ , both of which span the major fissiles, and is depleted through its decay and neutron-capture.

Solving Eq. 3 yields

$$N_L(t) = \left( N_{L0} - \frac{\vec{Z}_L \cdot \vec{\mathcal{F}}}{\tilde{\lambda}_L} \right) e^{-\tilde{\lambda}_L t} + \frac{\vec{Z}_L \cdot \vec{\mathcal{F}}}{\tilde{\lambda}_L}, \quad (4)$$

<sup>1</sup> In addition, one would group  $\Phi$  and  $\sigma$  by energy-groups, but we list the 1-group values for simplicity.

<sup>2</sup> We define the cooling time as the sum of all pure decay periods, including shutdowns.

<sup>3</sup> An exception to this is the  $^{135}\text{Xe}(n, \gamma)^{136}\text{Xe}$  cross-section.

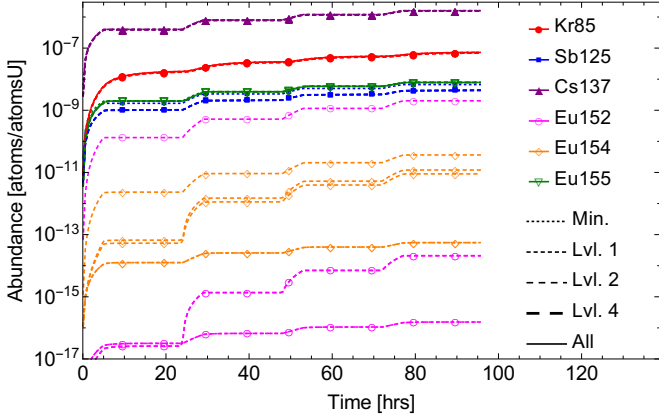


FIG. 1. Relative abundances of several fission fragments from a simulation of an irradiation history consisting of 4 [5, 19]hr ON/OFF periods and a thermal flux of  $\phi_t = 8.5 \times 10^{13} \text{ n/cm}^2/\text{sec}$  beginning with natural uranium. The simulation uses CINDER08 [31] cross-sections and the decay data was allowed to vary between ENDF7 [32], JEFF [33], and JENDL [34], with no observed difference. Linear fragments show no dependence on the layer of nuclear data. Color online.

with an initial nuclide abundance  $N_{L0}$ . We note that most linear fragments satisfy  $\tilde{\lambda}_L \approx \lambda_L$ , which can be verified by solving for the critical flux when decay and neutron channels have equal rates. Standard reactor fluxes are far below the critical fluxes of most fragments, ensuring that decay channels dominate. An exception to this is  $^{155}\text{Eu}$  and, in high thermal flux reactors [30],  $^{85}\text{Kr}$ . We include the effective decay constant in our derivations for generality. One can easily verify that our selected fragments are linear in nature using reactor simulations. We use a finite-difference methods solver for the interaction matrix, where the included nuclear data can be varied. A sample irradiation history is given by 4 cycles of [5, 19]hr ON/OFF periods and a thermal flux of  $\phi_t = 8.5 \times 10^{13} \text{ n/cm}^2/\text{sec}$ . The resulting relative abundances for our linear fragments and, for comparison, two non-linear fragments ( $^{152,154}\text{Eu}$ ) are shown in Fig. 1.

The minimum layer of nuclear data considered just our fragment of interest (FOI). This physically represents the case when each FOI is given by Eq. 4. Layer 1 added the  $\beta$ -parents. Layer 2 added the  $(n, \gamma)$  parent. Layer 4 included the primary, secondary, and (in some cases) tertiary  $(n, \gamma)$  channels as well as all of their  $\beta$ -parents with halflives greater than 30 sec. We also included a simulation of all nuclides with available data ( $\sim 700$ ). From Fig. 1, one can verify that  $^{85}\text{Kr}$ ,  $^{125}\text{Sb}$ ,  $^{137}\text{Cs}$ , and  $^{155}\text{Eu}$  are linear as they have very little dependence on the layer of nuclear data and, thus, are accurately given by Eq. 4. None of the fragments studied varied significantly between the major fission yields libraries [32–34].

To derive the cooling time diagnostic, we first expand Eq. 4 with  $\tilde{\lambda}T_{\text{irr}} \ll 1$  (criteria 1) and arrive at

$$N_L(t, T_c) = \Phi(\vec{Z}_L \cdot \vec{\Sigma}_{\text{fiss}}) e^{-\lambda_L T_c} + \mathcal{O}((\tilde{\lambda}_L T_{\text{irr}})^2), \quad (5)$$

once we have set  $N_{L0} = 0$ , accounted for the decay after a cooling time  $T_c$ , and separated the fission rate vector into a weighted fission cross-section and the flux through the relation  $\vec{F} = \vec{\Sigma}_{\text{fiss}}\phi$ . The expansion to arrive at Eq. 5 is easily valid for all fragments used here, except  $^{155}\text{Eu}$  which deviates from it by  $\sim 1 - 3\%$  due to its large cross-section. As  $\vec{\Sigma}_{\text{fiss}}$  is the fission cross-sections weighted by the fissile abundances, one can determine  $\vec{\Sigma}_{\text{fiss}}$  with similar chemical analyses as those used for the fragments [14].

Universally setting  $N_{L0} = 0$  appears to exclude cases with multiple irradiation cycles. Suppose we have a distribution of irradiation and cooling times described in Fig. 2, where  $t$  and  $\tau$  are the total irradiation and cooling times across all cycles. We recursively insert Eq. 4

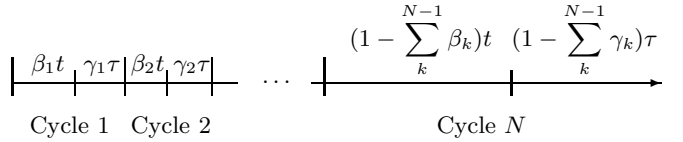


FIG. 2. Generalized irradiation history with  $N$  cycles, each consisting of an irradiation time of length  $\beta_i t$  and cooling time  $\gamma_i \tau$  with multiplicative factors  $\beta_i$  and  $\gamma_i$  that sum to unity. The  $N^{\text{th}}$  cycle is the remainder of the total irradiation time  $t$  and cooling time  $\tau$  with time ascending from left to right.

into itself as an initial condition for the following irradiation and cooling period to verify that distributing the total irradiation and cooling time in a generalized way is a negligible effect on our linear fragments. We find that the final activity ( $\alpha_L = \lambda_L N_L$ ) of a purely linear fragment (i.e.  $\tilde{\lambda}_L = \lambda_L$ ) with a generic distribution of  $t$  and  $\tau$  over  $N$  cycles is given by

$$\alpha_L(t, \tau, \vec{\beta}, \vec{\gamma}, N_{L0}) = (\lambda_L N_{L0} - \vec{Z}_L \cdot \vec{\mathcal{F}}) e^{-\lambda_L(t+\tau)} + (\vec{Z}_L \cdot \vec{\mathcal{F}}) e^{-\lambda_L \tau} \times f(\vec{\beta}, \vec{\gamma}), \quad (6)$$

with a pre-irradiation initial abundance  $N_{L0}$  and the function  $f(\vec{\beta}, \vec{\gamma})$  is given as a sum and product of exponentials over the additional  $N - 1$  cycles

$$f(\vec{\beta}, \vec{\gamma}) = \left( \prod_{i=1}^{N-1} e^{\lambda_L \gamma_i \tau} \right) + e^{-\lambda_L t} \times \sum_{i=1}^{N-1} \left[ \left( \prod_{j=1}^i e^{\lambda_L \beta_j t} \right) \left( \prod_{k=1}^{i-1} e^{\lambda_L \gamma_k \tau} \right) - \left( \prod_{j=1}^i e^{\lambda_L (\beta_j t + \gamma_j \tau)} \right) \right]. \quad (7)$$

This complex function for  $N$  cycles reduces to unity when  $N = 1$ . One can show that criteria 1, and the fact that the individual elements of  $\vec{\beta}$  and  $\vec{\gamma}$  are limited by unitarity, restricts Eq. 7 to very small deviations from 1. We analyzed generic values for  $\vec{\beta}$  and  $\vec{\gamma}$  within our expected  $t$  and  $\tau$  ranges and found that Eq. 7 is well-constrained to  $\lesssim 1\%$  deviations from unity. An exception to this is  $^{125}\text{Sb}$ , which showed larger deviations when the decay

time is concentrated towards earlier cycles (i.e. when  $\gamma_1 \gg \gamma_{k>1}$ ), but this is disfavored for our samples. As no fragments are expected in pre-irradiated fuel, we determine that  $N_{L0} = 0$  is a valid assumption at the start of irradiation and any subsequent cooling time diagnostic will now include intermediate shutdowns.

With  $N_{L0} = 0$ , the final abundance of a linear fragment can be expressed as in Eq. 5. A ratio of the activities of two linear fragments removes the explicit dependence on  $\Phi$  and creates the expression

$$\alpha_{n,d}(\vec{\Sigma}_{\text{fiss}}, T_c) = \frac{\lambda_n \vec{Z}_n \cdot \vec{\Sigma}_{\text{fiss}}}{\lambda_d \vec{Z}_d \cdot \vec{\Sigma}_{\text{fiss}}} e^{-(\lambda_n - \lambda_d)T_c}, \quad (8)$$

which is a direct measure of the total cooling time. One can correct Eq. 8 with higher order expansion terms to account for linear fragments with large neutron-capture components, but this will create a dependence on  $T_{\text{irr}}$ . For large fast fluences,  $\Phi$  must remain in Eq. 8 so as to account for fast fissions:  $\Phi_g \times (\vec{Z}_n^g \cdot \vec{\Sigma}_{\text{fiss}}^g)$ , with an implied sum over the neutron energy groups  $g$ .

As mentioned previously, the final value of  $\vec{\Sigma}_{\text{fiss}}$  is known from a measurement of fissile isotopes. However,  $\vec{\Sigma}_{\text{fiss}}$  varies over the irradiation period. Therefore, one must average the weighted fission cross-sections so as not to bias Eq. 8 towards U or Pu fissions. The averaging is conducted linearly over the fluence  $\Phi$  because  $T_{\text{irr}}$  is unknown. One can use the thermal fluence derived from Eq. 2 as the fluence endpoint and the initial value of  $\vec{\Sigma}_{\text{fiss}}$  reflected natural uranium for our samples [14]. This fluence-averaged value  $\langle \vec{\Sigma}_{\text{fiss}} \rangle_\Phi$  becomes a critical factor when predicting fragments that have cumulative yields with large plutonium components.

Inverting Eq. 8 reveals the cooling time diagnostic

$$T_c = \frac{1}{\lambda_d - \lambda_n} \ln \left( \frac{\alpha_{n,d} \lambda_d \vec{Z}_d \cdot \langle \vec{\Sigma}_{\text{fiss}} \rangle_\Phi}{\lambda_n \vec{Z}_n \cdot \langle \vec{\Sigma}_{\text{fiss}} \rangle_\Phi} \right). \quad (9)$$

Due to the pole in Eq. 9, two linear fragments with similar decay constants  $\lambda_n \simeq \lambda_d$ , such as a ratio of  $^{90}\text{Sr}$  and  $^{137}\text{Cs}$ , can produce large errors in the cooling time, but there are theoretical methods for removing these [35]. For fragments with large cross-sections, one can expand Eq. 4 to  $\mathcal{O}((\tilde{\lambda} T_{\text{irr}})^2)$ , but this introduces an unverifiable value for  $T_{\text{irr}}$  and only corrects the cooling time by a few percent.

#### IV. VERIFICATION

In Sec. II and Sec. III, we listed diagnostics for the thermal fluence and cooling time. These diagnostics were verified with the use of the reactor simulation described in Sec. III. Over 70 sample cases were evaluated with layer 4 nuclear data to determine the validity of the analytical calculations. The cases spanned a range of reasonable values for the thermal flux  $\phi_t$ , cooling time  $T_c$ , fast flux  $\phi_f$ , irradiation time  $T_{\text{irr}}$ , number of shutdowns

$N_s$ , and shutdown length  $T_s$ . The derived values for  $\Phi$  and  $T_c$ , using Eq. 2 and Eq. 9, were compared with those used as input to the simulation. We found that the only parameter that affected the fluence diagnostic is the introduction of a fast flux  $\phi_f$  as it slightly increases the final  $\rho$  and  $\epsilon$  values, which could be mistaken for a larger thermal fluence. Using the maximum expected fast flux, the diagnostic of Eq. 2 returned the input fluence within  $\sim 0.5\%$  for both the  $^{235}\text{U}/^{238}\text{U}$  and  $^{236}\text{U}/^{235}\text{U}$  ratios. The situation for the cooling time diagnostic was much more complicated.

We used the following ratios for the cooling time diagnostic:  $^{137}\text{Cs}/^{155}\text{Eu}$  ( $\alpha_1$ ),  $^{137}\text{Cs}/^{125}\text{Sb}$  ( $\alpha_2$ ), and  $^{155}\text{Eu}/^{125}\text{Sb}$  ( $\alpha_3$ )<sup>4</sup>. The derived cooling time was found to vary with all major reactor parameters listed above. As the total  $\Phi_t$  increased, the errors on Eq. 9 increased linearly, but this was shown to be mediated somewhat by the averaging of  $\vec{\Sigma}_{\text{fiss}}$ . The increase of  $\phi_f$  created an underestimation of  $T_c$  proportional to the additional fast cumulative yields of the fragments used in Eq. 9. Increasing the cooling time served to decrease the errors on all  $T_c$  diagnostics as the deviation from end-of-cycle activity ratios becomes more severe for longer  $T_c$ . Finally, the shutdown history is shown to have a very small impact, in agreement with the derivation in Sec. III. The maximum theoretical errors in percent for the expected reactor parameters and the largest overall theoretical error are provided in Tab. I.

	$\Phi$ Diagnostics		$T_c$ Diagnostics		
	$\epsilon$	$\rho$	$\alpha_1$	$\alpha_2$	$\alpha_3$
$\Phi_t$	$\sim 0\%$	$\sim 0\%$	3.86%	0.57%	-3.27%
$\phi_f$	0.54%	0.24%	-0.47%	-0.19%	-0.14%
$T_c$	0%	0%	-0.99%	-0.12%	0.89%
$N_s$	0%	0%	0.10%	0.01%	-0.10%
$T_s$	0%	0%	-0.17%	-0.16%	-0.14%
Overall	$\pm 0.54\%$	$\pm 0.24\%$	$\pm 4.02\%$	$\pm 0.63\%$	$\pm 3.40\%$

TABLE I. Theoretical errors for the fluence ( $^{235}\text{U}/^{238}\text{U}$  and  $^{236}\text{U}/^{235}\text{U}$  ratios) and cooling time ( $\alpha_1 = ^{137}\text{Cs}/^{155}\text{Eu}$ ,  $\alpha_2 = ^{137}\text{Cs}/^{125}\text{Sb}$ , and  $\alpha_3 = ^{155}\text{Eu}/^{125}\text{Sb}$  ratios) diagnostics given by Eq. 2 and Eq. 9. Each cell shows the maximum expected error over a particular reactor parameter (the thermal fluence  $\Phi_t$ , fast flux  $\phi_f$ , cooling time  $T_c$ , number of shutdowns  $N_s$ , and length of shutdowns  $T_s$ ) range. The overall theoretical error is the individual errors summed in quadrature, which provides a conservative maximum.

Overall, from Tab. I, one can see that the diagnostics derived in Eq. 2 for the fluence have extremely small theoretical errors and one can expect the correct fluence within  $\sim 0.5\%$ . For the cooling time diagnostic, the theoretical errors are more substantial as the fragment systems are more complex. Overall, one can expect the correct cooling time within  $\sim 4\%$ ,  $\sim 0.6\%$ , and  $\sim 3.4\%$  for

<sup>4</sup> Diagnostics using  $^{85}\text{Kr}$  were removed as it may have experienced volatile leakage.

the  $^{137}\text{Cs}/^{155}\text{Eu}$ ,  $^{137}\text{Cs}/^{125}\text{Sb}$ , and  $^{155}\text{Eu}/^{125}\text{Sb}$  ratios, respectively. The linear-averaging in Sec. III returned the lowest errors, but ignores the quadratic behavior of  $^{239}\text{Pu}$  at low burnup. We verified that removing  $^{239}\text{Pu}$  fissions and calculating Eq. 9 to  $\mathcal{O}((\tilde{\lambda}T_{\text{irr}})^2)$  can effectively eliminate these errors. We note that these errors are strictly theoretical and contain no systematic errors, such as fractionation or experimental uncertainties. We have also calculated the expected  $^{239}\text{Pu}$  abundance using a similar analytical method with errors of  $\sim 0.25\%$ , but this requires knowledge of many reactor parameters, so we have excluded it from our analysis. The theory errors of Tab. I are lower than the experimental measurement errors. With these notes in mind, we use these diagnostics to determine the thermal fluence and extract information about systematic errors from three cooling time diagnostics.

## V. EXPERIMENTAL APPLICATION

Ten archived samples were analyzed for their U and Pu isotopes, as well as the activities of several fission fragments. The actinides were separated and measured as described in Ref. [14]. In short, U metal or  $\text{UO}_3$  samples are dissolved in  $\text{HNO}_3$ , then loaded and separated on anion exchange columns to achieve separation of Pu from U. Isotope ratios and isotope dilution measurements were determined by TIMS. Fission fragments were measured by gamma spectrometry [15]. Samples H and K were in  $\text{UO}_3$  form, while the remainder were uranium metal.

Both fluence diagnostic methods were attempted, but discrepancies were observed between the  $^{236}/^{235}\text{U}$  and  $^{235}/^{238}\text{U}$  ratios in very-low burnup cases as shown in Fig. 3. The fluences determined in samples D through

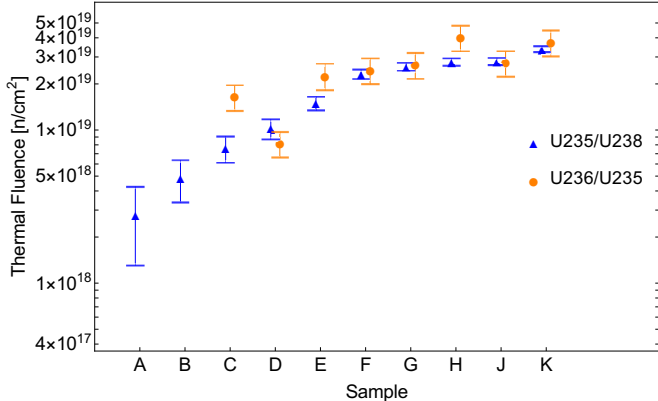


FIG. 3. The derived thermal fluence for ten experimental samples. The derivation for the thermal fluence used both the  $^{235}/^{238}\text{U}$  (triangles) and  $^{236}/^{235}\text{U}$  (circles) ratios and these methods are self-consistent in higher fluence samples. The  $^{236}/^{235}\text{U}$  diagnostic could not be used in samples with trace  $^{236}\text{U}$  amounts. Errors are the  $1\sigma$  errors from experimental measurements and theoretical estimates summed in quadrature. Color online.

K were all nearly self-consistent. Sample C reported fluences that deviate more strongly. Samples A and B were contaminated with  $^{236}\text{U}$  memory effects, so their values were not used. The chemical analyses of the remaining samples were conducted at a later time, correcting the  $^{236}\text{U}$  issue. Overall, it appears that our method of extracting the thermal fluence via Eq. 2 is accurate and self-consistent for the majority of samples with  $\Phi \geq 10^{19} \text{ n/cm}^2$ . Below this limit, the low concentrations of  $^{236}\text{U}$  created experimental difficulties in acquiring the fluence with multiple methods. Thus, one can determine the thermal fluence with two independent diagnostics in samples with appreciable amounts of  $^{236}\text{U}$ , but must rely solely on the  $^{235}/^{238}\text{U}$  ratio in extremely low-burnup samples with trace levels of  $^{236}\text{U}$ . The  $\epsilon$  diagnostic is only valid when  $\epsilon_0$  is known, so the  $\rho$  diagnostic should be used if enough  $^{236}\text{U}$  is present. The average error between the two diagnostics was 19.9%.

In determining the total cooling time, we used the ratios identified in Sec. IV. Figure 4 illustrates the agreement and tension between the different diagnostics. A few samples performed relatively well, but most demonstrated disagreement between the three cooling time diagnostics. In particular, the  $^{155}\text{Eu}$ -based determinations

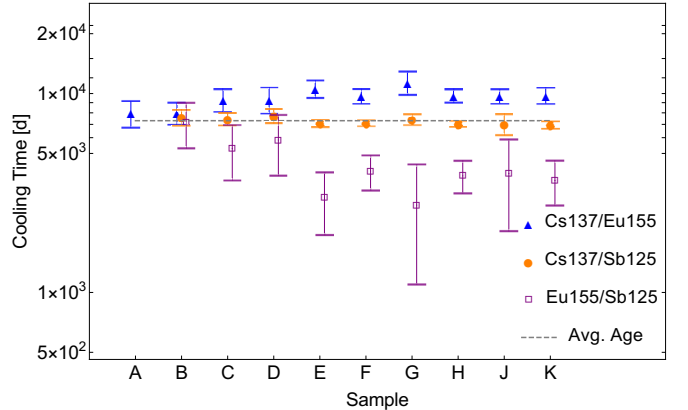


FIG. 4. The derived cooling times for ten experimental samples. The derivation of the cooling time used 3 ratios,  $\alpha_1$  (triangles),  $\alpha_2$  (circles), and  $\alpha_3$  (open squares). See text for definition. The average sample age of 20 yr is shown for comparison with the derived values. The errors are the  $1\sigma$  errors from the experimental measurements and theoretical estimates summed in quadrature. The disagreement between the diagnostics indicates the presence of systematic errors, which could be attributed to fractionation. Color online.

of  $T_c$  showed disagreement with the  $^{137}\text{Cs}/^{125}\text{Sb}$  ratio as the inferred fluence rises. Leakage of volatile fission fragments, such as  $^{85}\text{Kr}$ , can occur at the  $\gtrsim 13\%$  level in PWR fuels [36] so these ratios were removed. A portion of the bias from  $^{155}\text{Eu}$ -based diagnostics can be explained by the over-estimation of the  $^{239}\text{Pu}$ -component when linearly averaging  $\vec{\Sigma}_{\text{fiss}}$  and the need to compute  $T_c$  to second order, but these errors will only approach those in Tab. I. The  $^{137}\text{Cs}/^{125}\text{Sb}$  diagnostic seemed to match the average reported sample age of 20 yr. The  $^{125}\text{Sb}$  abun-

dance was not measured in sample A. The average diagnostic discrepancy was found to be  $\sim 37\%$  between the  $^{155}\text{Eu}$ -based diagnostics and the  $^{137}\text{Cs}/^{125}\text{Sb}$  ratio. The use of multiple  $T_c$  diagnostics allows one to detect the presence of systematic errors, such as fractionation, when diagnostics do not agree and a single consistent cooling time when they do. This technique must be used in the very low burnup regime as traditional same-species ratios are impractical.

## VI. CONCLUSION

The work conducted here demonstrates that the thermal fluence can be determined in low burnup samples using the  $^{235}\text{U}/^{238}\text{U}$  and  $^{236}\text{U}/^{235}\text{U}$  ratios. These ratios are common fluence diagnostics, which were verified with detailed reactor simulations and then experimentally demonstrated to be accurate and self-consistent when enough  $^{236}\text{U}$  is produced above the detection threshold. The average discrepancy between the two fluence diagnostics in our low burnup samples was 19.9% for  $\Phi > 10^{19} \text{ n/cm}^2/\text{sec}$ .

The low burnup of our reactor samples required new cooling time diagnostics to be derived, as the concentrations of standard diagnostic tags are below detection thresholds. The new cooling time diagnostics utilized simple linear fission fragments with long half-lives and considerable fission yields. Four such fragments were

identified and the derived diagnostics were verified in low burnup scenarios. The experimentally determined cooling times were shown to be consistent in some samples, but varied by  $\sim 37\%$  on average. In addition, leakage of volatile gases invalidated the diagnostics using  $^{85}\text{Kr}$ . Overall, the  $^{137}\text{Cs}/^{125}\text{Sb}$  ratio seemed to agree with the average sample age across all samples. Differing results for the cooling time, as measured by several diagnostics, proved to be indicative of systematic errors, such as fractionation, even in the very low burnup regime.

The fluence and cooling time derivation should be conducted in tandem, where the  $\Phi$  determination would be used to derive  $\langle \vec{\Sigma}_{\text{fiss}} \rangle_{\Phi}$  and verify that the sample has a burnup low enough to validate the simple analytical expressions for  $T_c$ . This work provides verification of fluence diagnostics and new cooling time diagnostic techniques to determine the presence of systematic errors in low burnup samples, both of which have applications in non-proliferation and verification.

## ACKNOWLEDGMENTS

We would like to thank the analytical chemistry team: L. Colletti, E. Lujan, K. Garduno, T. Hahn, L. Walker, A. Lesiak, P. Martinez, F. Stanley, R. Keller, M. Thomas, K. Spencer, L. Townsend, D. Klundt, D. Decker, and D. Martinez. Los Alamos National Laboratory supported this work through LDRD funding. This publication is LA-UR-16-26969.

---

- [1] A. V. Stepanov, T. P. Makarova, B. A. Bibichev, A. M. Fridkin, A. V. Lovtsyus, L. D. Preobrazhenskaya, A. A. Lipovskii, and A. N. Timofeev, Soviet Atomic Energy **49**, 673 (1980), ISSN 1573-8205.
- [2] T. W. Wood, B. D. Reid, J. L. Smoot, and J. L. Fuller, The Nonproliferation Review **9**, 126 (2002), <http://dx.doi.org/10.1080/10736700208436898>.
- [3] S. F. Boulyga and J. S. Becker, Journal of Analytical Atomic Spectrometry **17**, 1143 (2002).
- [4] S. F. Boulyga and K. G. Heumann, Journal of Environmental Radioactivity **88**, 1 (2006), ISSN 0265-931X.
- [5] J. S. Kim, Y. S. Jeon, S. D. Park, Y.-K. Ha, and K. Song, Nuclear Engineering and Technology **47**, 924 (2015), ISSN 1738-5733.
- [6] B. D. Reid, W. Morgan, E. Love Jr, D. Gerlach, S. Peterson, J. Livingston, L. Greenwood, and J. McNeece, Tech. Rep. (1999).
- [7] C. Gesh, PNNL-14568, February (2004).
- [8] A. Gasner and A. Glaser, Science and Global Security **19**, 223 (2011).
- [9] S. Caruso, M. Murphy, F. Jatuff, and R. Chawla, Annals of Nuclear Energy **34**, 28 (2007), ISSN 0306-4549.
- [10] S. Ansari, M. Asif, T. Rashid, and K. Qasim, Annals of Nuclear Energy **34**, 641 (2007), ISSN 0306-4549.
- [11] K. Mayer, M. Wallenius, and Z. Varga, Chemical Reviews **113**, 884 (2012).
- [12] I. Gauld and M. Francis (51 Annual Meeting of the Institute of Nuclear Materials Management (INMM), 2010).
- [13] A. C. Hayes and G. Jungman, Nucl. Instrum. Meth. **A690**, 68 (2012), 1205.6524.
- [14] B. Byerly, L. Tandon, A. Hayes-Sterbenz, P. Martinez, R. Keller, F. Stanley, K. Spencer, M. Thomas, N. Xu, and M. Schappert, Journal of Radioanalytical and Nuclear Chemistry (2015).
- [15] L. Tandon, K. Kuhn, P. Martinez, J. Banar, L. Walker, T. Hahn, D. Beddingfield, D. Porterfield, S. Myers, S. Lamont, et al., Journal of Radioanalytical and Nuclear Chemistry **282**, 573 (2009), ISSN 1588-2780.
- [16] H. Natsume, H. Umezawa, S. Okazaki, T. Suzuki, T. Sonobe, and S. Usuda, Journal of Nuclear Science and Technology **9**, 737 (1972).
- [17] R. Abernathy, G. Matlack, and J. Rein, *Sequential Ion Exchange Separation and Mass Spectrometric Determination of Neodymium, Uranium, and Plutonium in Mixed Oxide Fuels for Burnup and Isotopic Distribution Measurements*. (1972).
- [18] Marsh, S.F. and Ortiz, M.R. and Abernathy, R.M. and Rein, J.E., LA-5568 (1974).
- [19] A. Sánchez, F. Tomé, J. Bejarano, and M. Vargas, Nuclear Instruments and Methods in Physics Research Section A: Accelerators, Spectrometers, Detectors and Associated Equipment **313**, 219 (1992), ISSN 0168-9002.

- [20] J. Iturbe, *Applied Radiation and Isotopes* **43**, 817 (1992).
- [21] P. Huber and P. Jaffke, *Phys. Rev. Lett.* **116**, 122503 (2016), 1510.08948.
- [22] E. C. Freiling and M. A. Kay, *Nature* **209**, 236 (1966).
- [23] J. Navarro, R. Aryaeinejad, and D. Nigg, *Tech. Rep.* (2011).
- [24] B. Bergelson, A. Gerasimov, and G. Tikhomirov (2013).
- [25] Oak Ridge National Laboratory, *Scale: A Comprehensive Modeling and Simulation Suite for Nuclear Safety Analysis and Design*, Oak Ridge National Laboratory, 6th ed. (2011).
- [26] O. Meplan, *MURE, MCNP Utility for Reactor Evolution - User Guide - Version 1.0*, Report: LPSC 0912 (2009).
- [27] M. Pusa and J. Leppänen, *Nuclear science and engineering* **164**, 140 (2010).
- [28] H. Bateman, *Proc. Cambridge Philos. Soc.* **15**, 423 (1910).
- [29] A. Isotalo and P. Aarnio, *Annals of Nuclear Energy* **38**, 261 (2011), ISSN 0306-4549.
- [30] D. Ilas, *Tech. Rep.*, Oak Ridge National Laboratory (2012).
- [31] S. Holloway and W. Wilson, in *PSI Proceedings* (2008).
- [32] M. B. Chadwick et al., *Nucl. Data Sheets* **112**, 2887 (2011).
- [33] M. A. Kellett, O. Bersillon, and R. W. Mills, *The JEFF-3.1/-3.1.1 radioactive decay data and fission yields sub-libraries* (Nuclear Energy Agency, 2009).
- [34] K. Shibata, O. Iwamoto, T. Nakagawa, N. Iwamoto, A. Ichihara, S. Kunieda, S. Chiba, K. Furutaka, N. Otuka, T. Ohsawa, et al., *Journal of Nuclear Science and Technology* **48**, 1 (2011).
- [35] J. Cetnar, *Annals of Nuclear Energy* **33**, 640 (2006), ISSN 0306-4549.
- [36] Metz. V et. al., *Characterisation of spent nuclear fuel samples and description of methodologies and tools to be applied in FIRST-Nuclides*, CP-FP7-295722 (2013).